



## On Numerical Integration of Sea Bed Logging EM Models

Allen Q. Howard, Jr. ,

INSTITUTO DE GEOCIÊNCIAS,

PROGRAMA DE PÓS-GRADUAÇÃO EM GEOFÍSICA, Universidade do Pará

Copyright 2011, SBGf - Sociedade Brasileira de Geofísica.

This paper was prepared for presentation at the Twelfth International Congress of the Brazilian Geophysical Society, held in Rio de Janeiro, Brazil, August 15-18, 2011.

Contents of this paper were reviewed by the Technical Committee of the Twelfth International Congress of The Brazilian Geophysical Society and do not necessarily represent any position of the SBGf, its officers or members. Electronic reproduction or storage of any part of this paper for commercial purposes without the written consent of The Brazilian Geophysical Society is prohibited.

### Abstract

**This paper presents an alternative method to evaluate numerically the Fourier-Bessel integrals occurring in many electromagnetic field models used in the interpretation of geophysical data. In particular the interest is in the sea-bed-logging layered earth problem with a horizontal electric dipole (HED) in an anisotropic media when the lateral coordinate  $\rho$  is large (on the order of 10 km) resulting in highly oscillatory integrals that are difficult to evaluate numerically. The method replaces the real axis integration with a mathematically equivalent complex contour integration that converges exponentially when the product of the integration variable  $\lambda$  and the horizontal coordinate  $\rho$  is large. Example computations are made for the three components of the electric field for a standard form of the one-dimensional HED layered earth model. Analytic and numerical forms are compared for the primary fields and show good agreement.**

### Introduction

Computation of the electromagnetic fields of layered one dimensional models for dipole and loop sources involve numerical integration of Fourier-Bessel transforms with Bessel functions of order 0 and 1. For moderate distances scaled in skin depths, the integrands are usually smooth and do not have many oscillations before convergence is reached. In such cases simple real axis integration using for example Gauss-Legendre quadrature is adequate. However there are important cases for interpretation of measured geophysical data with distances of several skin depths, where the integrands can be highly oscillatory. In particular, in the case of sea bed logging, the horizontal coordinate separation  $\rho$  between transmitter and receiver locations can be over 10 km requiring source frequencies on the order of 1 Hz. The Fourier Bessel integrands have exponential convergence in the vertical coordinate  $z$ , but to have maximum range, the vertical separation between the transmitter and receivers on the sea-bed floor are kept small, on the order of 20 m.

In this situation the integrands are highly oscillatory with a slowly decreasing envelope. The real axis integration

is equivalent to summing numerically a slowly convergent alternating series. Since each succeeding term of alternating sign is only slightly smaller than the preceding term, the round off error can be significant when thousands of terms are summed in order to achieve sufficient convergence. One method to approach this type of problem is to apply special oscillating quadrature formulas. An early classic example of this type of quadrature is known as Filon's method (Abramowitz and Stegun, 1964). Filon used quadratic interpolation, Simpson's rule, to interpolate the kernel function  $h(x)$  between sample points to increase the accuracy of the integration of Fourier transform factor oscillatory factor  $e^{ikx}$ . A cubic interpolation oscillatory quadrature algorithm is also available (Press et. al. 1986). A more sophisticated oscillating quadrature method has been developed (Ting and Luke, 1981).

A popular and efficient method for numerical evaluation of Fourier-Bessel transforms uses fast Hankel transforms (Anderson, 1982). The resulting filters contain the Bessel function evaluations and are manipulated by exponential transform into a convolutional form. These techniques are efficient and with care can be used with oscillating integrands.

The approach here is to reduce the significant length real axis interval necessary to achieve numerical convergence by moving the numerical integration into the complex plane.

### Fourier-Bessel Transform Numerical Integration

In cases where the receiver antennas have relatively large separation horizontally from the transmitter, the Fourier-Bessel integrands of the scattered potentials are highly oscillatory making them difficult to evaluate by conventional quadrature formulas. In such cases, it is advantageous to deform the real axis integration into the complex  $\lambda$  plane. The transform integrals have the form

$$I_n(z, \rho) = \int_0^{\infty} F_n(\lambda, z) J_n(\lambda \rho) \lambda d\lambda, n = 1, 2 \quad (1)$$

where the kernel function has the symmetry  $F_n(-\lambda, z) = -(-1)^n F_n(\lambda, z)$ . Then it is possible to represent the transform integral in the form

$$I_n(z, \rho) = 1/2 \int_{-\infty}^{\infty} F_n(\lambda, z) H_n^{(1)}(\lambda \rho) \lambda d\lambda, \quad (2)$$

where the Hankel function of the first kind and order  $n$  has the asymptotic behavior (when  $|\lambda \rho| \gg 1$  and  $-\pi < \arg(\lambda \rho) < 2\pi$ )

$$H_n^{(1)}(\lambda \rho) \approx \sqrt{2/(\pi \lambda \rho)} e^{i(\lambda \rho - n\pi/2 - \pi/4)}. \quad (3)$$

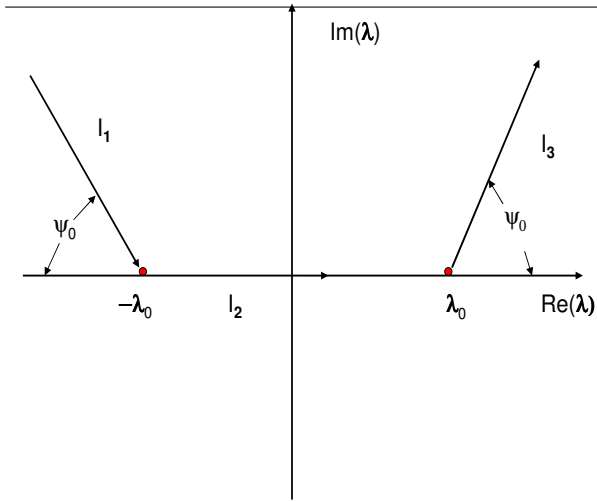


Figure 1: Three segment complex contour integration  $\Gamma = I_1 + I_2 + I_3$  with ray elevation angle  $\psi_0$  in the  $\lambda$  plane.

The idea is not new, for example a similar method has been used before (Anderson et. al. 1986) and others. This method differs in that the ray elevation angle  $\psi_0$  depends on the values of the coordinates  $\rho$  and  $z$ . To determine  $\psi_0$ , note that the exponential behavior of the Fourier-Bessel integrals for the up-going factor  $e^{iu_n z}$ , when the magnitude of the integration variable  $\lambda$  is large with respect to the magnitude of the intrinsic wavenumbers is

$$I(\lambda) = e^{i\lambda\rho - \lambda z} \quad (4)$$

Let  $z = R \sin \theta$ ,  $\rho = R \cos \theta$ , where  $R = (\rho^2 + z^2)^{1/2}$ . On contour segment  $I_3$  let the integration variable  $\lambda$  be given by

$$\lambda = \lambda_0 + e^{i\psi_0} s, \quad (5)$$

where  $s$  is real and positive. Then it follows that for the choice

$$\psi_0 = \pi/2 - \theta, \quad (6)$$

the exponential factor in equation (5) has maximum convergence, i.e.

$$I(\lambda) = I(\lambda_0) e^{-Rs}. \quad (7)$$

This choice of angle  $\psi_0$  is the asymptotic limit of the steepest descent path and in this sense is optimal. Similar results follow for the three other exponential factors  $e^{-iu_n z}$ ,  $e^{iv_n z}$  and  $e^{-iv_n z}$ . Thus one replaces the real axis integration by deformation into the upper-half  $\lambda$  plane. If this entails crossing branch cuts or poles of the integrand, they must be included. Fig. 1 shows the complex contour integration path  $\Gamma = I_1 + I_2 + I_3$ . By choosing real segment  $I_2$  end points  $\pm\lambda_0$  to the right and left respectively of integrand singularities and branch cuts, the ray paths  $I_1$  and  $I_3$  are equivalent, by Cauchy's integral theorem, to their real axis counterparts.

On the ray segments  $I_1$  and  $I_3$  the integrand decays exponentially and end points are chosen such that the integrand is less than a set tolerance. The upper limit on rays is chosen such that the value of the exponential part of the integrands are equal to  $1.0 \times 10^{-7}$ . As practical examples, consider the three electric field components of a HED in an  $N$  layer anisotropic media. From results similar to Xiong (Xiong, 1989), the Fourier-Bessel representation of these are given by

$$E_{nx}^{(s)}(\mathbf{x}) = \frac{\omega \mu_0 I_0 d \ell}{4\pi k_{hm}^2} \left[ \frac{-\cos 2\phi}{\rho} \int_0^\infty [k_{hm}^2 (a_n^{(+)} e^{iu_n z} + a_n^{(-)} e^{-iu_n z}) + iv_n \lambda^2 (b_n^{(+)} e^{iv_n z} - b_n^{(-)} e^{-iv_n z})] J_1(\lambda \rho) d\lambda + \right. \\ \left. - \sin^2 \phi k_{hm}^2 \int_0^\infty (a_n^{(+)} e^{iu_n z} + a_n^{(-)} e^{-iu_n z}) J_0(\lambda \rho) \lambda d\lambda + \cos^2 \phi \int_0^\infty iv_n \lambda^2 (b_n^{(+)} e^{iv_n z} - b_n^{(-)} e^{-iv_n z}) J_0(\lambda \rho) \lambda d\lambda \right],$$

$$E_{ny}^{(s)}(\mathbf{x}) = \frac{\omega \mu_0 I_0 d \ell}{4\pi k_{hm}^2} \sin 2\phi \int_0^\infty [k_{hm}^2 (a_n^{(+)} e^{iu_n z} + a_n^{(-)} e^{-iu_n z}) + iv_n \lambda^2 (b_n^{(+)} e^{iv_n z} - b_n^{(-)} e^{-iv_n z}) (J_0(\lambda \rho)/2 - \frac{J_1(\lambda \rho)}{\lambda \rho})] \lambda d\lambda,$$

$$E_{nz}^{(s)}(\mathbf{x}) = \frac{\omega \mu_0 I_0 d \ell}{4\pi k_{hm}^2} \cos \phi \kappa_n^2 \int_0^\infty \lambda^4 (b_n^{(+)} e^{iv_n z} + b_n^{(-)} e^{-iv_n z}) J_1(\lambda \rho) d\lambda. \quad (8)$$

These representations are a consequence of the two component magnetic vector representations

$$A_x(\mathbf{x}) = \frac{i\mu_0 I_0 d \ell}{4\pi} \int_0^\infty [a_n^{(+)}(\lambda) e^{iu_n z} + a_n^{(-)}(\lambda) e^{-iu_n z}] J_0(\lambda \rho) \lambda d\lambda,$$

$$A_z(\mathbf{x}) = \frac{i\mu_0 I_0 d \ell}{4\pi} \frac{\partial}{\partial x} \int_0^\infty [b_n^{(+)}(\lambda) e^{iv_n z} + b_n^{(-)}(\lambda) e^{-iv_n z}] J_0(\lambda \rho) \lambda d\lambda - \frac{iu_n}{\lambda^2} a_n^{(+)}(\lambda) e^{iu_n z} + \frac{iu_n}{\lambda^2} a_n^{(-)}(\lambda) e^{-iu_n z} J_0(\lambda \rho) \lambda d\lambda, \quad (9)$$

where

$$u_n = \sqrt{k_{hm}^2 - \lambda^2}, \quad \text{Im}(u_n) \geq 0, \quad (10) \\ v_n = \sqrt{k_{hm}^2 - \kappa_n^2 \lambda^2}, \quad \text{Im}(v_n) \geq 0,$$

and the horizontal and vertical intrinsic layer wavenumbers are

$$k_{hm} = (i\mu_0 \omega \sigma_{hm})^{1/2}, \quad \text{Im}(k_n) \geq 0. \quad (11) \\ k_{vn} = k_{hm} / \kappa_n.$$

where  $\mu_0$  is the magnetic permeability of free space,  $\omega = 2\pi f$  is the circular frequency in rad/s,  $\sigma_{hm}$  is the  $n^{\text{th}}$  layer horizontal conductivity in S/m, and the  $n^{\text{th}}$  layer anisotropic index is

$$\kappa_n = (\sigma_{hn} / \sigma_{vn})^{1/2} \quad (12)$$

The Fourier-Bessel amplitudes  $(a_n^{(\pm)}(\lambda), b_n^{(\pm)}(\lambda))$  are determined by matching tangential field components at the

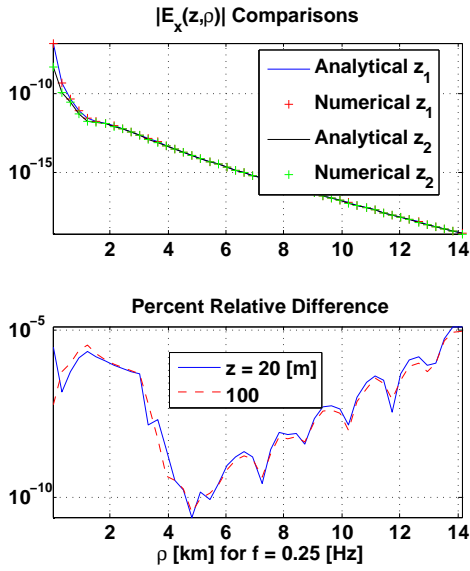


Figure 2: Comparison of Analytic and Numerical forms of  $E_x^{(p)}(\rho, z)$  for parameters given by equation (15).

boundaries. For purposes here it is sufficient to note that the primary field coefficients for a HED antenna are known to be

$$\begin{aligned} a^{(0+)}(\lambda) &= e^{-iu_{ns}z_T}/u_{ns}, \\ a^{(0-)}(\lambda) &= 0, \\ b^{(0+)}(\lambda) &= ie^{-iv_{ns}z_T}/\lambda^2, \\ b^{(0-)}(\lambda) &= 0. \end{aligned} \quad (13)$$

This choice of coefficients when substituted in equation (8) is the Fourier-Bessel representation of the primary electric field. The primary electric field has the explicit analytic form

$$\begin{aligned} E_x^{(p)}(\mathbf{x}) &= \frac{i\omega\mu_0 I_0 d \ell}{4\pi k_h^2} \left[ \frac{e^{ik_h R}}{R} (k_h^2 \sin^2 \phi - ik_h R \cos 2\phi / \rho^2) + \kappa \cos 2\phi \frac{e^{ik_v R a}}{R^3} (1 + ik_v R a \kappa^2 (z - z_T)^2 / \rho^2) - \kappa \cos^2 \phi \frac{e^{ik_v R a}}{R_a^3} (ik_v R_a^3 - R_a^2 - \kappa^2 (z - z_T)^2 (k_v^2 R_a^2 + 3ik_v R_a - 3)) \right], \\ E_y^{(p)}(\mathbf{x}) &= \frac{-i\omega\mu_0 I_0 d \ell}{4\pi k_h^2} \sin 2\phi \left[ ik_h \frac{e^{ik_h R}}{R} (1/\rho^2 - ik_h / (2R)) - \kappa \frac{e^{ik_v R a}}{2R_a^3} (3 - ik_v R a \kappa^2 \frac{(z - z_T)^2}{R_a^2} - (3 - 3ik_v R a - k_v^2 R_a^2 - 2ik_v R_a^3 / \rho^2)) \right], \\ E_z^{(p)}(\mathbf{x}) &= \frac{-i\omega\mu_0 I_0 d \ell}{4\pi k_h^2} \kappa (z - z_T) \rho \cos \phi \frac{e^{ik_v R a}}{R_a^3} [3i\kappa^2 k_v R a - 3\kappa^2 + k_h^2 R_a^2]. \end{aligned} \quad (14)$$

Computation and comparison of representations (8) and (14) for typical sea-bed-logging geometries (Eidesmo, 2002) provides a good test of accuracy of the numerical integration as well as the consistency of the Fourier-Bessel

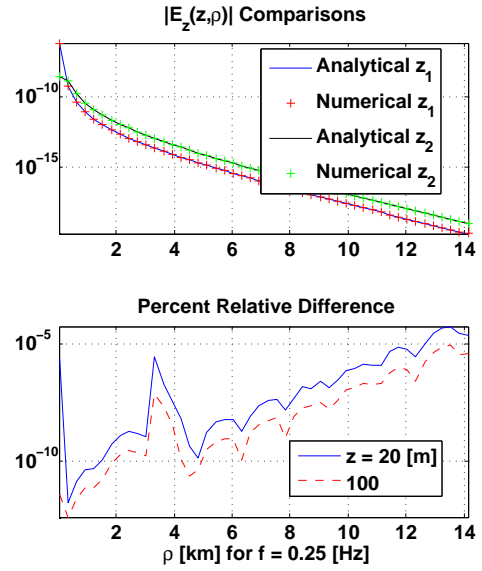


Figure 3: Comparison of Analytic and Numerical forms of  $E_y^{(p)}(\rho, z)$  for parameters given by equation (15).

transform and analytic forms of the field representations. The following comparisons use parameters

$$\begin{aligned} f &= 0.25 \text{ [Hz]} \\ I_0 d \ell &= 1 \text{ [Amp - m]} \\ z_T &= 0 \text{ [m]} \\ \sigma_h &= 4 \text{ [S/m]} \\ \kappa &= 2 \text{ [unitless]}. \end{aligned} \quad (15)$$

The angle with respect to the  $\text{real}(\lambda)$  axis of contour segments  $I_1$  and  $I_3$  is chosen to be the non-optimal but constant value  $\pi/3$ . The optimum values depend on both  $\rho$  and  $z$ . The examples here use 256 Gauss-Legendre quadrature points on the real axis segment and 512 points on the complex ray segments.

### Summary and Conclusions

This paper presents a simple alternative method to efficiently evaluate Fourier-Bessel transforms numerically with possible highly oscillatory integrands. The numerical integration uses a simple contour consisting of three straight line segments in the complex  $\lambda$  plane. The elevation angle  $\psi_0$  of the first and last segments can be chosen asymptotic to the steepest descent path and in this sense the contour is asymptotically optimal. Example computations of HED electric field components for a layered anisotropic model show at least 6 significant figures of accuracy for radial offsets of up to 14 km.

### References

Abramowitz, M., and I. A. Stegun, 1965, Handbook of Mathematical Functions: Dover Publications,

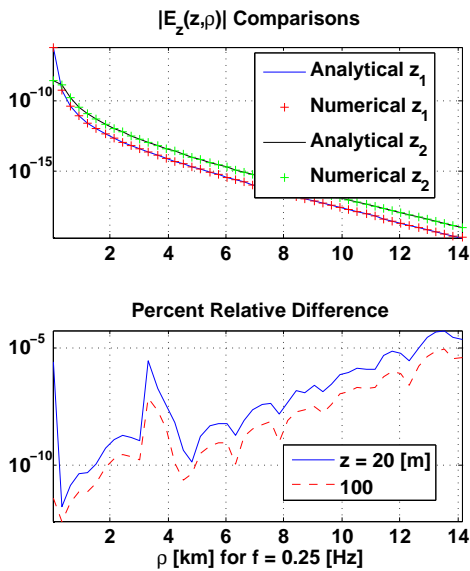


Figure 4: Comparison of Analytic and Numerical forms of  $E_z^{(p)}(\rho, z)$  for parameters given by equation (15).

Ting, B. Y., and Luke, Y., 1981, Computation of integrals with oscillatory and singular integrands: *Math. Comp.*, **37**, p169-183

Press, W. H., et. al., *Numerical Recipes*, Second Edition, Cambridge University Press, p577-583

Anderson, W. L., 1982, Fast Hankel Transforms Using Related and Lagged Convolutions, *ACM Transactions on Mathematical Software*, vol. 8, No. 4, p344-368,

Xiong, Z., 1989, Electromagnetic fields of electric dipoles embedded in a stratified anisotropic earth, *Geophysics*, vol. 54, no. 12, p1643-1646

Anderson, B., K. A. Safinya, and T. Habashy, 1986, Effects of Dipping Beds on the Response of Induction Tools, *Society of Petroleum Engineers*, 61st Annual Tech. Conference, New Orleans, paper no. SPE 15488

Eidesmo, T., S. Ellingsrud, L. M. MacGegor, S. Constable, M. C. Sinha, S. Johansen, F. N. Kong, and H. Westerdahl, 2002, Sea Bed Logging (SBL), a new method for remote and direct identification of hydrocarbon filled layers in deep water areas, *fast break*, vol 20, p144-152

### Acknowledgments

I thank my colleagues Professors Cicero Roberto Teixeira Rêgis, Marcos Welby Corrêa da Silva and João Batista Corrêa da Silva at the INSTITUTO DE GEOCIÊNCIAS, FACULDADE DE GEOFÍSICA, Universidade do Pará for their efforts in facilitating this opportunity to again participate in geophysical research and teaching in Brazil.